Transition zone in controlling spatiotemporal chaos

Jihua Gao,[1] Lingling Xie,[1] Wei Zou,[2,3] and Meng Zhan[2,*]
[1]*Shenzhen Key Laboratory of Special Functional Materials, College of Materials, Shenzhen University, Shenzhen 518060, China*
[2]*Wuhan Institute of Physics and Mathematics, Chinese Academy of Sciences, Wuhan 430071, China*
[3]*Graduate School of the Chinese Academy of Sciences, Beijing 100049, China*
(Received 14 January 2009; published 14 May 2009)

The controllability of spatiotemporal chaos is investigated. Contrary to our common sense that there is only one transition point (i.e., a critical control strength) for successful control, we find that actually a *transition zone* exists, connecting two transition points for the local and global stabilities of the controlled state, respectively. Within the zone, the controllable probability increases from zero to one for random initial conditions. This behavior is found to be very generic and is expected to have a severe consequence in realistic applications in the control of spatiotemporal chaos.

DOI: 10.1103/PhysRevE.79.056214 PACS number(s): 05.45.Gg, 47.27.Rc

Chaos control has become one of central problems in the field of nonlinear science [1]. Spatiotemporal systems [2–4] have multiple spatial degrees of freedom and could present complex oscillations and rich patterns, which naturally appear in electronic circuits, optical, plasmas, chemical, and biological systems as well. Therefore, the control of spatiotemporal chaos with the aim to drive the controlled system to our target state closely connects to realistic applications and is certainly of great significance. So far, various control approaches such as the local pinning control [5,6], the time-delay feedback control [7], the adaptive method [8], and the forcing in Fourier space [9] and in wavelet subspace [10] have been proposed in order to realize a successful control and achieve a high efficiency. On the other hand, an important problem of controllability of spatiotemporal chaos has also been theoretically studied recently [11–15]. It is found that in a certain spatiotemporal system (e.g., the flow turbulent system in incompressible Navier-Stokes equations), the whole velocity field can only be partially controlled through the pinning control of one component of the velocity field even in the limit of long control time and strong control strength [13,14]. In this work, we will address another relevant problem about the controllability of spatiotemporal chaos: the impact of initial conditions. One may intuitively believe that to realize control, a threshold with a sufficiently large control strength (denoted by ε_c with ε representing our control parameter) is needed; namely, only if $\varepsilon > \varepsilon_c$, a control can succeed, and otherwise it cannot. Thus, a dichotomy of control parameter is generally expected. Our study, however, surprisingly shows that a transition zone staying at a finite width of control parameter exists, which connects two critical parameters for uncontrollability and full controllability for random initial conditions. The phenomenon appears due to the intrinsic character of spatiotemporal chaotic states, the spatiotemporal complexity.

Consider the following one-dimensional (1D) complex Ginzburg-Landau equation (CGLE):

$$\partial_t A = A + (1 + ic_1)\partial_x^2 A - (1 + ic_2)|A|^2 A, \tag{1}$$

where $A = A(x,t)$ is complex variables and c_1 and c_2 are the real system parameters. Equation (1) describes the general characteristics at the onset of a Hopf bifurcation of spatiotemporal systems and is the most studied model of spatiotemporal chaos. If the periodic boundary condition is imposed, system (1) admits the following traveling wave solutions:

$$A(x,t) = A_0 e^{i(kx - wt + \theta)}, \tag{2}$$

where $A_0 = \sqrt{1-k^2}$, $w = c_2 + (c_1 - c_2)k^2$, and $k = \frac{2m\pi}{L}$, with L representing the system size and m being an integer. θ is a constant phase (without losing generality, we set $\theta = 0$). These solutions are linearly stable against long-wavelength perturbations if

$$k^2 < k_E^2 = \frac{1 + c_1 c_2}{2(1 + c_2^2) + 1 + c_1 c_2} \tag{3}$$

holds [2,16]. Thus if $1 + c_1 c_2 < 0$ [the so-called Benjamin-Feir (BF) unstable region], all plane-wave solutions [Eq. (2)] are unstable, and the system exhibits various spatiotemporal chaotic behaviors including defect turbulence (DT) and phase turbulence (PT). DT is characterized by the behavior that the fluctuations of amplitude become dominant over the phase dynamics, and PT is opposite.

We perform a global control approach by injecting a periodic signal into the original system, and hence we modify Eq. (1) to the controlled form

$$\partial_t A = A + (1 + ic_1)\partial_x^2 A - (1 + ic_2)|A|^2 A + \varepsilon(\hat{A} - A), \tag{4}$$

where ε is the feedback control intensity and $\hat{A}$ is the target signal chosen from one of the periodic traveling waves of Eq. (2). Similar techniques have been used in the control of the CGLE in one, two, and three dimensions. See, e.g., Refs. [17–19] and numerous others. Without losing generality, we choose $m = 2$ as the target state throughout this paper; clearly the study can be extended to other choice of m. It is notable that $A = \hat{A}$ is already a solution of system [Eq. (4)], and the effect of control simply changes the stability of the solution—from unstable to stable. Also note that now the

*Corresponding author; zhanmeng@wipm.ac.cn

control intensity ε is the only control parameter.

To study the stability of the solution $A=\hat{A}$, in what follows we conduct the linear stability analysis. We consider the system variable has a small deviation from the target signal and therefore has the form $A=A_0[1+a(x,t)]e^{i[kx-wt+\varphi(x,t)]}$, in which $a(x,t)$ and $\varphi(x,t)$ are the small deviations from the amplitude and phase of the target state. Inserting the above system variable into Eq. (4) and considering $|a|\ll 1$ and $|\varphi|\ll 1$, we obtain

$$a_t = a_{xx} - 2kc_1a_x - 2(1-k^2)a - c_1\varphi_{xx} - 2k\varphi_x - \varepsilon a,$$

$$\varphi_t = c_1a_{xx} + 2ka_x - 2c_2(1-k^2)a + \varphi_{xx} - 2kc_1\varphi_x - \varepsilon\varphi, \quad (5)$$

where $a_t=\partial_t a$, $a_x=\partial_x a$, $a_{xx}=\partial_x^2 a$, and φ_t, φ_x, φ_{xx} have the similar forms. The eigenfunction of Eq. (5) can be written as

$$\begin{pmatrix} a \\ \varphi \end{pmatrix} = \begin{pmatrix} a_0 \\ \varphi_0 \end{pmatrix} e^{(\sigma t+ipx)}, \quad (6)$$

where σ is complex and the wave number of the perturbation $p=\frac{2m'\pi}{L}$ is real (m' is an integer). Considering Eq. (5), we have

$$\sigma = \frac{1}{2}(F_{11}+F_{22}) + \frac{1}{2}\sqrt{(F_{11}-F_{22})^2 + 4F_{12}F_{21}}, \quad (7)$$

with

$$F_{11} = -p^2 - i2kc_1p - 2(1-k^2) - \varepsilon,$$

$$F_{12} = c_1p^2 - i2kp,$$

$$F_{21} = -c_1p^2 + i2kp - 2c_2(1-k^2),$$

$$F_{22} = -p^2 - i2kc_1p - \varepsilon.$$

Denote $\lambda=\mathrm{Re}(\sigma)$ and $\Omega=\mathrm{Im}(\sigma)$ with Re and Im representing the real and imaginary parts of variable, respectively. $\sigma=\lambda+i\Omega$. Obviously the sign of λ determines the stability of the controlled state; namely, if λ is positive, the small deviation will explode with time; but oppositely if λ is negative, it will shrink. Observing Eq. (7), we find that λ linearly decreases with ε (i.e., $\lambda\propto-\varepsilon$) and Ω is independent of ε. The value of λ depends on the system parameters c_1 and c_2, the wave number k of the target ($k=\frac{2m\pi}{L}$ with $m=2$), which is fixed in the controlling, and the wave number p of the perturbation ($p=\frac{2m'\pi}{L}$).

In Fig. 1(a), we show the relation between λ and ε for different m' by numerically calculating λ in Eq. (7). For specificity, we choose the system parameters $c_1=2.1$ and $c_2=-1.5$ (within the DT regime). $L=100$. For each m', there is a critical value $\varepsilon_c(m')$, corresponding to the ε at the crossing-zero λ position of the $\varepsilon-\lambda$ straight line. Obviously, the maximum value of $\varepsilon_c(m')$ could theoretically guarantee the stability of the target state against any small perturbations. Figure 1(b) exhibits the dependence of $\varepsilon_c(m')$ on m', which well indicates that the $m'=9$ mode is the most unstable mode and its corresponding $\varepsilon_c(\varepsilon_c\approx 0.29)$ should be the critical control parameter.

Below let us test this theoretical prediction by numerical simulations. We integrated the controlled CGLE [Eq. (4)] directly with random initial conditions of A [both $\mathrm{Re}(A)$ and $\mathrm{Im}(A)$ are chosen within $(-1,1)$] and checked the computational stability by adjusting space iterations and time steps. The system evolves from $t=-1000$ and the control is switched on at $t=50$. The control probability versus ε is shown in Fig. 2(a). Interestingly, we find that the control results are actually sensitively influenced by different initial conditions, and the system is not always controllable even if $\varepsilon>\varepsilon_c$. With increasing ε, the controllable probability monotonically increases, and the system can always be controlled if ε is larger than the other critical strength ($\varepsilon\approx 0.53$). As a result, for different initial conditions, a transition zone (not a single transition point) appears, starting from one threshold for the local stability and ending at the other one for the global stability. In the paper, we denote these two thresholds with $\varepsilon_1(\varepsilon_1=\varepsilon_c)$ and ε_2, respectively.

To quantify the control effects and show the average distance between the system variable and the target state, we define a function

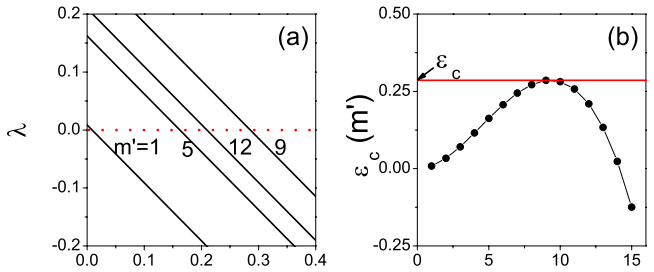

FIG. 1. (Color online) (a) The dependence of λ on ε for different m'. $m'=1$, 5, 9, and 12, for illustration. (b) The dependence of the critical strength $\varepsilon_c(m')$ on m'. $c_1=2.1$, $c_2=-1.5$, $L=100$, and $m=2$.

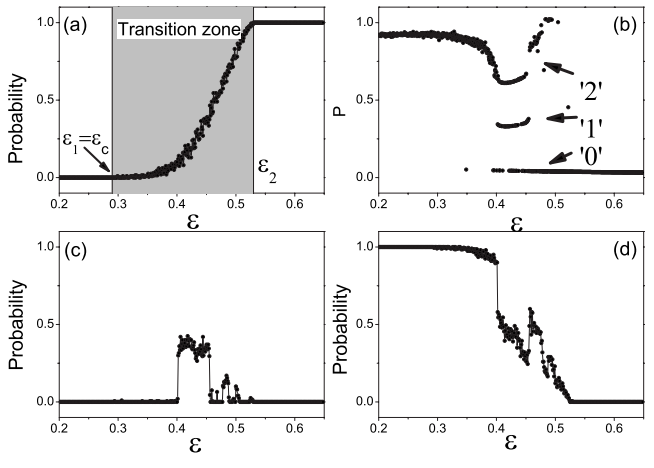

FIG. 2. (a), (c), and (d) The appearance probabilities for different random initial conditions for the states 0, 1, and 2, respectively. For the controllable state in (a), a transition zone appears, connecting two transition points ε_1 ($\varepsilon_1=\varepsilon_c$) and ε_2 for the local and global stability parameters, respectively. (b) The plot of P vs ε, showing multiple values within $\varepsilon_1<\varepsilon<\varepsilon_2$. See the text for more details.

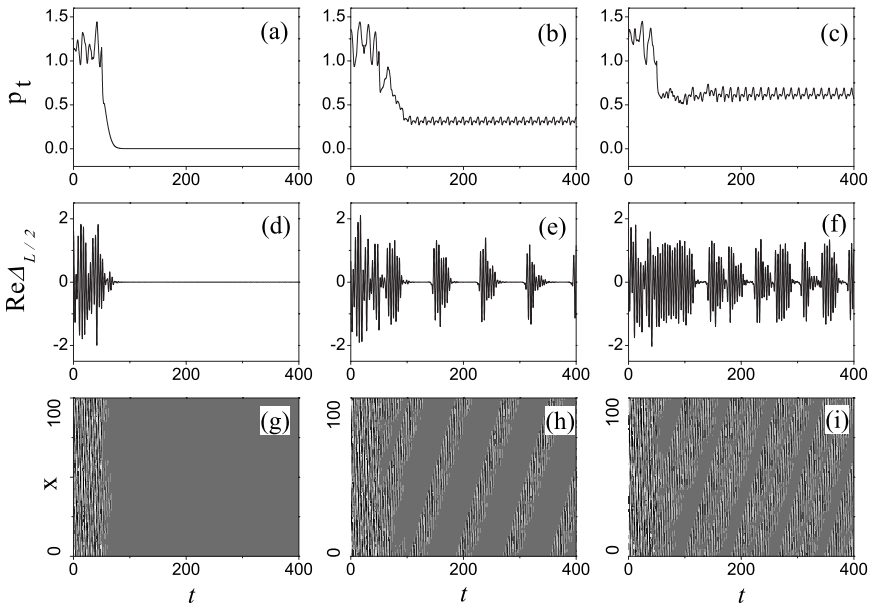

FIG. 3. The time evolutions of P_t, Re $\Delta_{L/2}$, and Re Δ are shown in the up, middle, down rows, respectively. The three columns correspond to the three different states 0, 1, and 2, respectively. In (h) and (i), the behavior of defect-induced intermittency with a roughly periodic structure is obvious.

$$P = \lim_{\Delta T \to \infty} \frac{1}{\Delta T} \int_0^{\Delta T} dt \frac{1}{L} \int_0^L |\Delta(x,t)| dx,$$

with $\Delta(x,t)=A(x,t)-\hat{A}(x,t)$ indicating the instant difference. If the system is completely controlled, P drops to zero (or nearly zero), and otherwise P remains a large value. Figure 2(b) shows P versus ε. In numerics, a very large ΔT has been chosen and larger ΔT does not change the result. We notice that the patterns within the region $\varepsilon \in [\varepsilon_1, \varepsilon_2]$ are rather complicated, clearly with different groups of P values. We may denote these different behaviors with different numbers, as shown the numbers 0, 1, 2 in Fig. 2(b). Clearly the number 0 represents the controllable state, and the numbers 1 and 2 represent the uncontrollable states. Numerically we set $P<0.1$ as the "0" state, $0.1<P<0.5$ as the "1" state, and $P>0.5$ as the "2" state. Their corresponding probability distributions for the states 1 and 2 are illustrated in Figs. 2(c) and 2(d), respectively.

To study the details of these three states, we plot the time evolutions of $P_t(P_t=\frac{1}{L}\int_0^L |\Delta(x,t)|dx)$, Re $\Delta_{L/2}$ ($\frac{L}{2}$ denotes the middle point of the pattern), and the patterns of Re Δ in the three rows of Fig. 3, respectively. The three columns of Fig. 3 correspond to these three states, respectively, $\varepsilon=0.42(\varepsilon_1<\varepsilon<\varepsilon_2)$. Different from the state 0 with the difference vanishing after a short time, for the state 1, the system can be occasionally synchronized with the target state but shows short deviations intermittently. As a whole, it produces a finite average value P [Fig. 2(b)]. Roughly this intermittent behavior is periodic, which is obvious from all three panels of the second column. As shown in Fig. 3(h), the straight drifting of one difference zone makes the intermittent phenomenon globally and periodically exist and so the whole system uncontrollable. More detailed study shows that this intermittency is induced by the remaining defect point within the difference zones, and locally it is not completely periodic due to the existence of defect point. Thus we may call it defect-induced intermittency. To the best knowledge of ours, this defect-induced intermittency with a roughly periodic behavior has never been addressed before. For the state 2, clearly there are two difference zones [Fig. 3(i)] with the same drifting velocity, which naturally make the value of P larger. For much larger P [e.g., the scattered data at about $\varepsilon=0.47$ in Fig. 2(b)], more complicated patterns are possible.

To show the robustness and generality of this effect, next we select one identical initial state, which has well evolved to a defect turbulent state, set different θ from 0 to 2π in Eq. (2) as our target state and recalculate P. This manipulation will not change the result of stability analysis but will conveniently show the sensitivity of initial conditions. The result is shown in Fig. 4 with the recovered three values for the controllable 0 state and two uncontrollable 1 and 2 states. The seemly random distribution of P on θ clearly shows that the control effect is highly sensitive on the set of initial conditions, which thus can be believed to be unavoidable in any control of spatiotemporal chaos. For other initial conditions, the result is qualitatively unchanged. We have also investigated the effect of system size and found that if the system size is sufficiently large (e.g., $L=100$ used in the paper), the

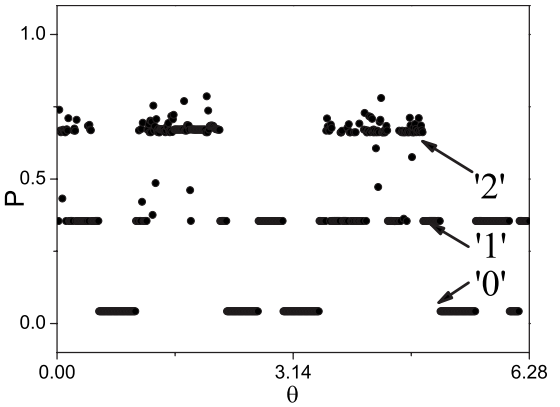

FIG. 4. The plot of P vs θ, showing the sensitivity of control effects on initial conditions.

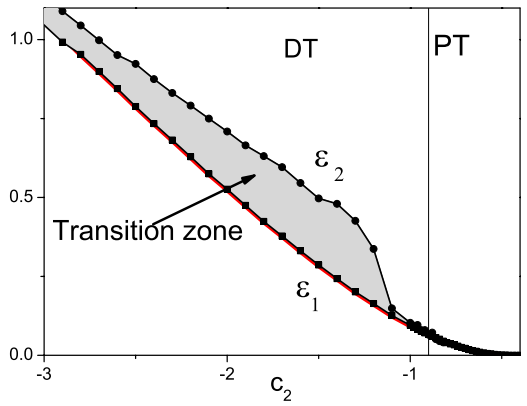

FIG. 5. (Color online) The plots of ε_1 and ε_2 as a function of the system parameter c_2. $c_1=2.1$. The letters "DT" and "PT" denote the defect turbulent and phase turbulent regions, respectively. The behavior of transition zone can be generally observed in a very broad parameter range, as shown the gray part within the defect turbulent regime in the picture.

values of ε_1 and ε_2 (and the location of transition zone) are nearly unchanged with different L. In addition, we have studied the impact of system parameters. This time the parameter $c_1=2.1$ is fixed and c_2 is scanned from -3 to 0. According to the previous studies on the 1D CGLE [4,20,21], at the parameter $c_2\approx-0.9(c_1=2.1)$, the DT will transit to PT. We find that the behavior of transition zone persists within the whole DT parameter region (Fig. 5). This finding suggests that we always need a much larger driving strength to realize a control for random initial conditions or several additional times of test if the control parameter is within the transition zone. Again the first critical parameter ε_1 from numerical simulations (squares) is identical to the theoretically predicted value from the linear stability analysis ε_c (solid red line). After the DT-PT transition point, the two values of ε_1 and ε_2 begin to coincide and the usual one transition point behavior survives. This can be intuitively understood. As now within the PT region, the condition for the occurrence of the defect-induced intermittency does not exist; a long observation time can always make the target state, which is locally stable, be globally stable, and thus the collapsing of a transition zone with two separate transition points to a transition point. Note that around the BF critical parameter ($c_2\approx-0.48$), we find that a finite critical control strength is needed again. Nevertheless, it is not interesting from the chaos control point of view.

In conclusion, we have studied the controllability of spatiotemporal chaos (particularly the defect turbulent chaos) both theoretically and numerically, uncovered an unusual effect of initial conditions, and discovered a dynamical phenomenon, the defect-induced intermittency, in the control. Interestingly, the controllability of spatially extended systems is found to be a probability event for different initial conditions, and it shows that the controllability is harder to achieve than what is expected previously. Due to the occurrence of the defect-induced quasiperiodic intermittency, which can be believed as attractor of systems in some way, the controlled system can keep uncontrollable for any long time. As we cannot always set the initial conditions being extremely close to the target state, and in some circumstance we even do not know the exact information of the target state, we have to carefully consider this effect in any realistic applications of controlling spatiotemporal chaos. Finally, we hope that all these results are observable and applicable to other spatiotemporal systems and control methods.

This work was partially supported by the Outstanding Oversea Scholar Foundation of Chinese Academy of Sciences (Bairenjihua) and the National Natural Science Foundation of China under Grant No. 10675161.

[1] There are vast references in the literature on the chaos control. For recent development, see, e.g., S. Boccaletti, C. Grebogi, Y.-C. Lai, H. Mancini, and D. Maza, Phys. Rep. **329**, 103 (2000); A. S. Mikhailov and K. Showalter, *ibid.* **425**, 79 (2006); a Theme Issue in Phil. Trans. R. Soc. A **364**, 2269 (2006) and references therein.
[2] Y. Kuramoto, *Chemical Oscillations, Waves, and Turbulence* (Springer, Berlin, 1984).
[3] M. Cross and P. Hohenberg, Rev. Mod. Phys. **65**, 851 (1993).
[4] I. Aranson and L. Kramer, Rev. Mod. Phys. **74**, 99 (2002).
[5] J. H. Xiao, G. Hu, J. Z. Yang, and J. H. Gao, Phys. Rev. Lett. **81**, 5552 (1998).
[6] L. Junge and U. Parlitz, Phys. Rev. E **61**, 3736 (2000).
[7] M. E. Bleich and J. E. S. Socolar, Phys. Rev. E **54**, R17 (1996); W. Just, T. Bernard, M. Ostheimer, E. Reibold, and H. Benner, Phys. Rev. Lett. **78**, 203 (1997).
[8] S. Sinha and N. Gupte, Phys. Rev. E **58**, R5221 (1998).
[9] S. J. Jensen, M. Schwab, and C. Denz, Phys. Rev. Lett. **81**, 1614 (1998).
[10] G. W. Wei, M. Zhan, and C.-H. Lai, Phys. Rev. Lett. **89**, 284103 (2002).
[11] G. Franceschini, S. Bose, and E. Scholl, Phys. Rev. E **60**, 5426 (1999).
[12] J. Bragard and S. Boccaletti, Phys. Rev. E **62**, 6346 (2000).
[13] S. G. Guan, Y. C. Zhou, G. W. Wei, and C.-H. Lai, Chaos **13**, 64 (2003).
[14] S. G. Guan, G. W. Wei, and C.-H. Lai, Phys. Rev. E **69**, 066214 (2004).
[15] A. Ahlborn and U. Parlitz, Phys. Rev. E **77**, 016201 (2008).
[16] B. Janiaud, A. Pumir, D. Bensimon, V. Croquette, H. Richter, and L. Kramer, Physica D **55**, 269 (1992).
[17] M. Jiang, X. Wang, Q. Ouyang, and H. Zhang, Phys. Rev. E **69**, 056202 (2004).
[18] X. He, H. Zhang, B. Hu, Z. Cao, B. Zheng, and G. Hu, New J. Phys. **9**, 66 (2007).
[19] L. Du, Q. Chen, Y.-C Lai, and W. Xu, Phys. Rev. E **78**, 015201(R) (2008).
[20] B. I. Shraiman, A. Pumir, W. van Saarloos, P. C. Hohenberg, H. Chate, and M. Holen, Physica D **57**, 241 (1992).
[21] H. Chate, Nonlinearity **7**, 185 (1994).